

High temperature mass spectrometric study of the vaporization behaviour of SiC–SiO₂ system

Gabriele Honstein*, Christian Chatillon, Francis Baillet

Laboratoire de Thermodynamique et Physico-Chimie Métallurgiques (UMR-5614, associée au CNRS-UJF/INPG) E.N.S.E.E.G. BP 75,
Domaine Universitaire, 38402 Saint Martin d'Hères, France

Received 18 September 2006; received in revised form 17 January 2007; accepted 24 January 2007
Available online 22 February 2007

Abstract

The study of the gaseous phase of different SiC–SiO₂ powder compositions with a high temperature mass spectrometer and a multiple cells device provides information about the evaporation behaviour of silicon carbide which serves as material for production of fine particle filters for diesel engines. We obtained a variation of the partial pressure values with a maximum for samples containing 30–45 mol% of SiO₂ in contrast to thermodynamic predictions. Some SiC powders were subjected to a heat treatment in order to obtain an oxide layer on the grain surfaces. Different times of heat treatment resulted in different CO(g) and SiO(g) pressures which at high temperature converged to the same values. Surprisingly, an excess of SiO₂ provoked a decrease of the SiO(g) pressure which was explained by taking into account two steady-state congruent vaporization processes in the effusion cell, one from SiC + SiO₂ and one from SiO₂.

© 2007 Published by Elsevier B.V.

Keywords: Inorganic materials; Gas–solid reactions; Thermodynamic properties

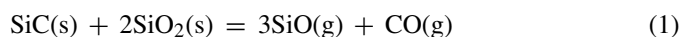
1. Introduction

The understanding of vaporization behaviour of the SiC–SiO₂ system is essential for the study of silicon carbide recrystallization. Previous studies [1,2] have shown that the material transport mainly takes place through the gaseous phase according to a so called vaporisation–condensation mechanism [2]. The reported study concerns some questions about the gaseous phase developed during vaporization of pure SiC + SiO₂ mixtures and its characterization using a combination of the Knudsen effusion technique and mass spectrometric measurements.

2. The SiO₂–SiC system

The SiO₂–SiC system is a section of the Si–0.5O₂–C ternary phase diagram presented in Fig. 1. The evaporation in this pseudo-binary section is known to be congruent, i.e. the gaseous phase composition is fixed for any composition of the solid and

follows the main reaction:



with the equilibrium constant

$$K_p = P^3(\text{SiO}) P(\text{CO}). \quad (2)$$

It follows from the Gibbs–Konovalow theorem [3] that for a fixed SiC/SiO₂ composition the total pressure will be an extremum for a system which has an indifferent (azeotropic or congruent) state. So:

$$P_{\text{tot}} = P(\text{SiO}) + P(\text{CO}) \quad (3)$$

Using (2):

$$P_{\text{tot}} = P(\text{SiO}) + \frac{K_p}{P^3(\text{SiO})} \quad (4)$$

And finally

$$\frac{dP_{\text{tot}}}{dP(\text{SiO})} = 1 - 3 \frac{K_p}{P^4(\text{SiO})} \quad (5)$$

with an extremum for

$$P(\text{SiO}) = 3P(\text{CO}) \quad (6)$$

* Corresponding author. Tel.: +33 476 82 65 50; fax: +33 476 82 67 67.
E-mail address: gabriele.honstein@ltpcm.inpg.fr (G. Honstein).

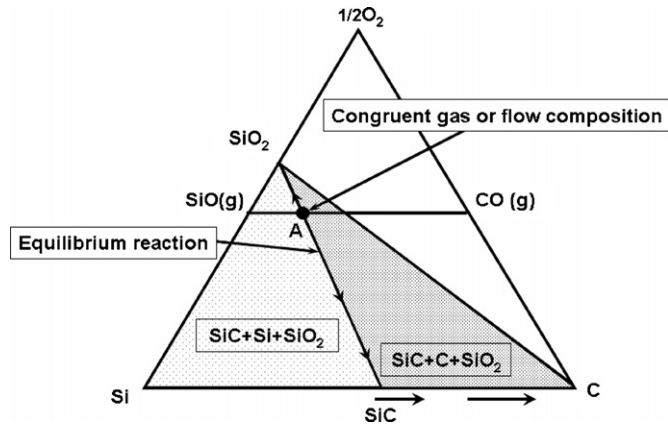


Fig. 1. Isothermal section of the Si–C–0.5O₂ ternary phase diagram at 1500 K. Identical phase equilibria are observed in the range of 1100–1650 K. Arrows show the evolution of condensed phase composition due to gas losses (CO and SiO) in equilibrium conditions.

For this indifferent state, which is an azeotropic state, the gaseous phase composition in the Si–C–O ternary system is (n_j is the number of j -atom in the gas phase):

$$x_{\text{Si}} = \frac{n_{\text{Si}}}{n_{\text{Si}} + n_{\text{C}} + n_{\text{O}}} = \frac{P(\text{SiO})}{P(\text{SiO}) + P(\text{CO}) + (P(\text{SiO}) + P(\text{CO}))} = \frac{3}{8} \quad (7)$$

$$x_{\text{C}} = \frac{n_{\text{C}}}{n_{\text{Si}} + n_{\text{C}} + n_{\text{O}}} = \frac{P(\text{CO})}{P(\text{SiO}) + P(\text{CO}) + (P(\text{SiO}) + P(\text{CO}))} = \frac{1}{8} \quad (8)$$

$$x_{\text{O}} = \frac{n_{\text{O}}}{n_{\text{Si}} + n_{\text{C}} + n_{\text{O}}} = \frac{P(\text{SiO}) + P(\text{CO})}{P(\text{SiO}) + P(\text{CO}) + (P(\text{SiO}) + P(\text{CO}))} = \frac{1}{2} \quad (9)$$

This composition is located at the intersection point of SiC–SiO₂ line with SiO–CO line shown in Fig. 1 as point A. Thus, whatever is the relative proportion of SiC and SiO₂, the condensed phase will produce gas of composition at A. In the case of gas losses in open systems only, any solid composition between pure SiC and A will move at equilibrium towards SiC.

In the case of congruent vaporization under vacuum [4] the ratio of flows is fixed according to:

$$\frac{dN_{\text{SiO}}/dt}{dN_{\text{CO}}/dt} = 3. \quad (10)$$

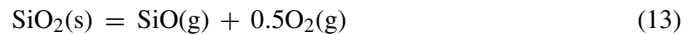
In this relation N_{SiO} and N_{CO} are the numbers of molecules of SiO and CO, respectively, which left the surface of the condensed phase under vacuum during the period of dt . The Hertz–Knudsen equation for flows is

$$\frac{dN_i}{dt} = \frac{P_i s C}{\sqrt{2\pi R M_i T}} \quad (11)$$

where C and s describe the geometry of the vaporization container [4], R the molar gas constant, M_i the molar mass of the gaseous molecule i and T is the temperature. For a condensed phase composition along the SiO₂–SiC line relations (10) and (11) lead to the following condition for the partial pressures ratio:

$$\frac{P(\text{SiO})}{P(\text{CO})} = 3.76 \quad (12)$$

The theoretical values of the equilibrium partial pressures of SiO(g) and CO(g) in our effusion cells were calculated using the equilibrium constant K_p , the condition for the congruent effusion flows given by (12) and thermodynamic data from the JANAF tables [5]. The same calculations were made for congruent vaporization of the pure SiO₂ that follows the main reaction:



The occurrence of minor reactions producing Si(g) and O(g) was included in these calculations in the high temperature range.

3. Experimental

The high temperature mass spectrometric device is a magnetic analyser (nuclide original, 12 in. radius) which has been fitted with

- (i) a multiple Knudsen cell furnace device [6],
- (ii) a restricted collimation of the molecular beam [7] optimized in order to discard any surface re-vaporisation detection of gaseous species coming from the orifice surroundings or thermal shields as already analyzed [8] and
- (iii) an in situ liquid nitrogen frozen ionisation chamber [9] in order to decrease the vacuum background peak at mass 28 at least by a factor of 100.

A “free floated” shutter is used to distinguish effusion flow from the background. Its midway location and its size as small as possible allow measurements without any perturbation by the background flow existing between the furnace and source housings. These conditions associated with the restricted-collimation-molecular-beam-sampling-device allow direct and reliable measurements of the so-called “permanent gases” [7], in the present case the CO(g) and N₂(g) molecules at mass 28. Measurements performed with the multiple Knudsen cell method have been recently reviewed in conjunction with the implementation of a new mechanical positioning device [10].

Measurements were performed with samples of different silicon carbide powder (High Purity SiC, Norton Saint-Gobain, Norway, $d_{50} = 0.5 \mu\text{m}$) and silica powder (Sipernat 350, Degussa) mixtures. Other samples were made by oxidation of SiC powder under air enriched with water vapour at 900 °C for 3, 10 and 30 h (samples 3, 10 and 30 h, respectively). To identify the composition of the effused gaseous phase of each cell – loaded with a specific sample – the intensities of SiO⁺ and CO⁺ ions present in the ionized molecular beam were monitored at ionisation energies of 20 and 48 eV, respectively. Measurements of samples containing silica were performed at a maximum temperature of 1650 K due to Knudsen flow limitations. Some parasitic species due to impurities in the powders (e.g. Na(g) from Na₂O in SiO₂) were detected at the beginning of the experiments up to 1450 K.

The samples were loaded in three cells of the multiple cell device, the fourth one served as reference. The cells used were tantalum cells with 2 mm orifice diameter and 2 mm orifice length (2 mm × 2 mm), the inner diameter of the cells being 16 mm.

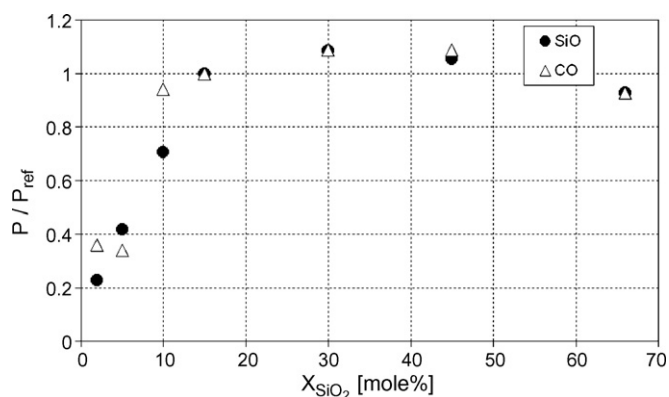


Fig. 2. Measured relative partial pressures of CO(g) and SiO(g) as a function of powder composition in the pseudo-binary SiC–SiO₂ section at 1650 K. The partial pressures of the mixture with 15 mol% SiO₂ are taken as reference (P_{ref}).

4. Results and interpretations

For the same gaseous species their measured ion intensity ratios are directly proportional to their partial pressure ratios. These pressure ratios display the dependency on the sample composition as presented in Fig. 2. The samples were referenced arbitrarily to the 15 mol% SiO₂ containing powder mixture. The pressure values of SiO(g) and CO(g) are not constant and the maximum value was obtained within the composition range of 30–45 mol% SiO₂.

The existence of a maximum in the diagram presented in Fig. 2 does not agree with thermodynamic behaviour (see Section 2), that predicts for congruent evaporation according to reaction (1) a gaseous phase of constant composition and pressure for a given constant temperature independent of the composition of the condensed phase. Otherwise, from a kinetic point of view, using the extent of reaction (or reaction coordinate defined by Prigogine and Defay [3]) and applying it to the reaction (1), this maximum was rather expected for a stoichiometric composition (i.e. 66 mol% SiO₂). However, this irregularity could come from the influence of the different number of contacts between the reacting SiC and SiO₂ powder grains on the vaporization rate.

Results from experiments performed with oxidized powders compared to a 15 mol% SiO₂ powder mixture as reference are presented in Fig. 3 which shows smoothed diagrams of experimental partial pressures deduced from our measured ionic intensities and the weight loss calibration of the mass spectrometer. The oxidized samples show clearly different evaporation regimes for low and high temperature regions (different slopes for the smoothed curves up to 1350 K and above 1380 K), while the evolution for the 15 mol% mixed powder reference sample shows a regular behaviour as expected in vaporization processes. The oxidized powders show significant differences compared to each other in the lower temperature region below 1470 K, and seem to vaporize with the same pressure values at higher temperatures. Another important observation is the position of the CO(g) pressure being above that of SiO(g), in contrast to thermodynamic predictions.

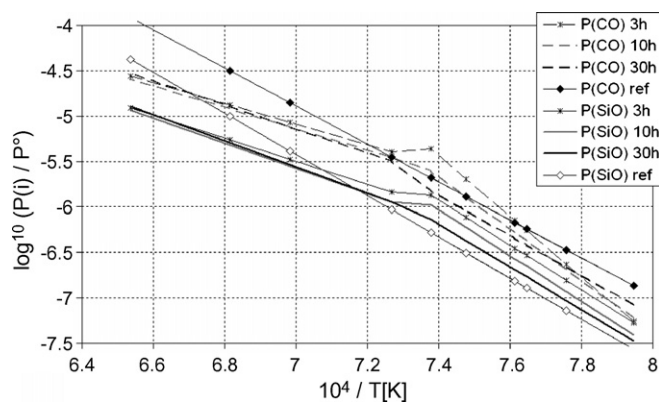


Fig. 3. Measured partial pressures (smoothed) as a function of the reciprocal temperature when heating SiC crystals, pre-treated for surface oxidation. The reference is a 15 mol% SiO₂ powder mixture (P^0 is the standard pressure; all pressures are in bar units).

Thermodynamic data from the JANAF tables [5] were used to calculate the equilibrium pressures for congruent vaporization. This helped to evaluate reactions which take place to produce the gaseous phase. Fig. 4 compares the resulting equilibrium partial pressures from these calculations with experimental values for one example. The $P(\text{SiO})$ and $P(\text{CO})$ from the experiments are a factor 20 and 3, respectively, smaller than the calculated pressures for the congruent vaporization according to reaction (1). The explanation for this behaviour are the net evaporation coefficients $\alpha(\text{SiO})$ and $\alpha(\text{CO})$, which are equal to 1 at equilibrium and lower than 1 when the vaporization is kinetically hindered [11], and which depend on temperature. The diffusion process through the SiO₂ layer on the SiC grains causes apparently retarded vaporization.

The non-equilibrium situation may be related to the tendency to independent vaporization behaviour of two condensed systems: SiO₂ + SiC pseudo-binary and SiO₂ pure. These two systems vaporize at different oxygen potentials and a steady-state situation is reached in the effusion cell that can be measured with the mass spectrometer. In order to understand the evolution of SiO(g) and CO(g) partial pressures they were displayed as a function of oxygen potential in Fig. 5. With increasing oxygen potential, starting from the SiC + SiO₂ pseudo-binary, we

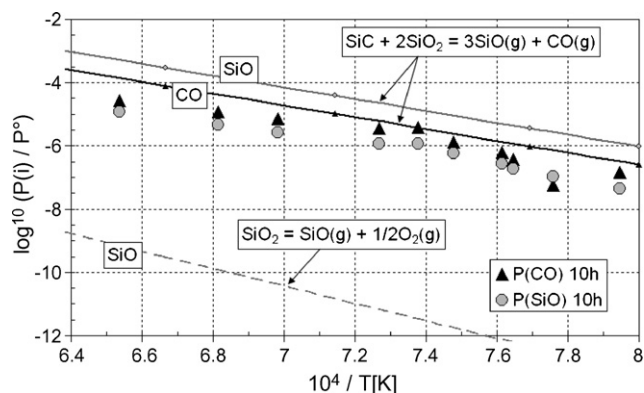


Fig. 4. Comparison of equilibrium partial pressures (calculated for the congruent SiC–SiO₂ vaporization) with measured values.

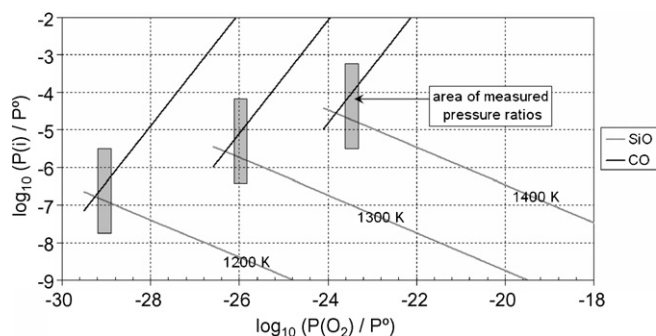


Fig. 5. Variation of calculated CO(g) and SiO(g) partial pressures for reaction (1) when the oxygen partial pressure increases from the value corresponding to congruent behaviour for the reaction (1) towards the value for congruent vaporization of pure SiO₂ at 1200, 1300 and 1400 K. Grey areas mark the ranges of oxygen potentials during experiments deduced from the measured $P(\text{CO})$ to $P(\text{SiO})$ ratios.

observe that CO(g) equilibrium partial pressure increases and SiO(g) decreases for equilibrium reaction (1). By passing their cross point we obtain $P(\text{CO})$ higher than $P(\text{SiO})$. This situation is exactly that we observed during our experiments.

The change in the partial pressure with temperature may be assigned to a structural change in the created SiO₂ layer. It may be the transition from high quartz to high cristobalite at (1079 ± 250) K [5].

Regarding CO(g) pressures in the low temperature region ($T < 1350$ K), it is clear that a thicker layer of SiO₂ inhibits the CO(g) evaporation coming from the interface and undergoing diffusion processes in the SiO₂ layer. However, at low temperature, until 1288 K, lower pressures of CO(g) for 3 and 10 h samples were observed compared to 30 h sample. An explanation could be a mechanical damage of the thicker SiO₂ layer (sample 30 h) due to thermal stress (micro cracks) during cooling after the heat treatment for the creation of the SiO₂ layer. These micro-cracks facilitate the CO-diffusion through this layer in the 30h sample. Rising temperature provokes “healing” of the micro-cracks and CO has to diffuse under similar conditions as in the 3 and 10 h samples through a thicker layer of SiO₂.

For SiO(g), the decrease of pressure with layer thickness cannot result a priori from a diffusion process in the SiO₂ layer. Assuming that 30 h oxidized grains have initially thicker SiO₂-layer than the 3 h one, the contribution of SiO(g) resulting from only SiO₂ decomposition (relation (13)), either from silica grains or from thick surface layers on SiC, should be less important than from interaction of SiO₂ with SiC (relation (1)) at the inner interface in contact with SiC grains. From the theoretical values for the SiC–SiO₂ interface (Fig. 4), the total SiO(g) pressure in a cell, which is a necessarily a steady-state value between the two different congruent states (reactions (1) and (13)), has to

decrease. This would explain lower experimental $P(\text{SiO})$ values for 30 h samples.

At high temperature all samples behave similarly, which can be explained with different modifications of each composition due to effusion losses and a tendency to steady-state vaporization with similar surface layers.

5. Summary

The observed partial pressures of SiO(g) and CO(g) are lower than the calculated equilibrium values which indicates either the presence of evaporation coefficients or shows that the studied system is in a non-equilibrium steady-state.

An excess of SiO₂, both in form of added powder or scale on the SiC grains, increases the oxygen partial pressure in the system and pushes it away from the azeotropic behaviour according to Eq. (1).

The oxidized samples tend to one preferential composition by the effusion of gases composed of appropriated amounts of SiO(g) and CO(g), irrespective of their initial composition. Their evaporation behaviour becomes similar in high temperature regions because of finally similar compositions and structure.

Acknowledgement

The authors acknowledge Saint Gobain CREE for sponsoring this study.

References

- [1] N.S. Jacobson, K.N. Lee, D.S. Fox, *J. Am. Ceram. Soc.* 75 (6) (1992) 1603–1611.
- [2] J. Kriegesmann, in: K. Ishizaki, K. Niihara, N. Isotani, R. Ford (Eds.), *Grain Boundary Controlled Properties of Fine Ceramics*, JFCC Workshop Series: Materials Proceeding and Design, Elsevier Applied Science, London, New York, 1992, pp. 176–188.
- [3] I. Prigogine, R. Defay, *Chemical Thermodynamics*, Longmans, London, 1965.
- [4] M. Heyrman, A. Pisch, C. Chatillon, *Proceedings CIEC 9*, Bardonecchia, Italy, September 5–7, 2004.
- [5] M.W. Chase Jr., *NIST-JANAF Thermochemical tables*, 4th ed., *J. Phys. Chem. Ref. Data*, Monograph 9, 1998.
- [6] C. Chatillon, L.F. Malheiros, P. Rocabois, M. Jeymond, *High Temp. High Press.* 34 (2002) 213–233.
- [7] P. Morland, C. Chatillon, P. Rocabois, *High Temp. Mater. Sci.* 37 (1997) 167–187.
- [8] C. Chatillon, M. Allibert, A. Pattoret, *High Temp. Sci.* 8 (1976) 233–255.
- [9] M. Tmar, C. Chatillon, *J. Chem. Thermodyn.* 19 (1987) 1053–1063.
- [10] M. Heyrman, C. Chatillon, H. Collas, J.-L. Chemin, *Rapid Commun. Mass Spectrom.* 18 (2004) 163–174.
- [11] G.M. Rosenblatt, in: N.B. Hannay (Ed.), *Treatise on Solid-State Chemistry VI. Surfaces*, Plenum Press, New York, 1976, pp. 165–239.